

# Filling Effect on the Structural, Electrical, and Magnetic Properties of PVAc/Co Composites

M. Abdelaziz<sup>1,2</sup>

<sup>1</sup>Department of Natural Science, Riyadh Community College, King Saud University, Riyadh 11437, Kingdom of Saudi Arabia

<sup>2</sup>Department of Physics, Faculty of Science, Mansoura University, Mansoura 35516, Egypt

Received 11 November 2009; accepted 2 February 2012

DOI 10.1002/app.36942

Published online in Wiley Online Library (wileyonlinelibrary.com).

**ABSTRACT:** Polyvinyl-acetate/-cobalt (PVAc/Co) composite films were prepared using a casting technique. The structural and physical properties were studied using X-ray diffraction (XRD), differential scanning calorimetry (DSC), Fourier transform infrared (FTIR) spectroscopy, dielectric measurements, direct current magnetic susceptibility ( $\chi_{dc}$ ), and electron spin resonance (ESR). The XRD patterns revealed that the incorporation of Co particles increases the amorphization of PVAc and Co oxide formations. The DSC results suggest that the thermal properties obviously improved. Frequency and filler concentration dependence of the dielectric constant ( $\epsilon'$ ) and AC conductivity ( $\sigma_{AC}$ ) were measured at room temperature in the frequency range 20 Hz to 3 MHz of pure PVAc and PVAc/Co composite films. The dielectric constant shows

usual dielectric dispersion behavior. The dielectric constant and AC conductivity increased with the increase in Co content. The variation of  $\sigma_{AC}$  is attributed to hopping of polarons and bipolarons in the composites. The filling level dependence of the effective magnetic moment ( $\mu_{eff}$ ) has been evaluated. The ESR spectra exhibit a peak of an increasing depth as Co content increases. The control of thermal stability, dielectric and magnetic moment of the composites films is interesting for applications such as electric and magnetic sensors. © 2012 Wiley Periodicals, Inc. *J Appl Polym Sci* 000: 000–000, 2012

**Key words:** composites; structural; DSC; dielectric; magnetic moment; ESR

## INTRODUCTION

Polymers have become increasingly attractive because of its large number of applications in applied and basic science. Conductive polymer composite (CPC) materials result from the mixture of conductive particles dispersed in an insulating phase. The filler is usually a metal powder, carbon black, fiber of carbon black, metal fibers, and so forth, whereas the insulating phase can be a thermosetting resin, thermoplastic, elastomer, and so forth. The composite material combines both the intrinsic properties of the fillers (mechanical, electrical, magnetic, and thermal) and of the matrix (elasticity, easy to manipulate, and low cost). The various conductive properties of CPC have allowed them to find a variety of industrial applications. They are used, for example, as protection devices against electromagnetic radiation and for the dissipation of electrostatic discharge<sup>1</sup>; they are also used in microelectronics as electrical conductive adhesive for electrical connections.<sup>2</sup> The control of the conductivity of CPC is also

interesting for applications including sensor, electrochromic devices, corrosion inhibitors, electrochemical actuators, electromagnetic shielding, polymeric batteries, etc.<sup>3,4</sup> The conductivity of these composites depends strongly on the nature and interaction of the filler with the polymeric matrix. Cobalt (Co) metal was selected as a filler due to its interesting electric and magnetic properties, because it may exist in different structural forms: tetrahedral, octahedral, and isolated forms.<sup>5</sup> Polyvinyl-acetate (PVAc) is often used as a primary ingredient for the formation of glue, which is odorless, nonflammable, and suitable for use at low temperatures [sensor and actuators]. PVAc-based composite materials are significantly manufactured by resin emulsifier, adhesive, paper, paint, and textile industries.<sup>6</sup>

This article focuses on the effect of Co addition on structural, electrical, and magnetical properties of PVAc.

## EXPERIMENTAL

### Sample preparation

PVAc and Co powder (99.99%, particle size = 63  $\mu\text{m}$ ) were purchased from Aldrich. The PVAc film and PVAc/Co composite films were fabricated by the solvent casting technique. At first, PVAc was dissolved

Correspondence to: M. Abdelaziz (mabdelaziz62@yahoo.com).

in benzene, and the solution was then stirred vigorously for 10 h. The necessary weight fractions of Co were first dispersed in benzene solution under sonication processor and then added gradually into the polymeric solution with continuous stirring. To improve the dispersion of Co in polyvinyl acetate solution, ultrasonicator at a frequency of 20 kHz for 10 min was used. Finally, the homogenous PVAc/Co dispersion was poured out onto leveled glass plates and evaporated slowly in air to form a PVAc/Co composite film. Solid films were obtained after solvent evaporation and drying of samples in vacuum oven. The filler concentration  $W$  (wt %) was calculated from the following equation:

$$W(\text{wt } \%) = \frac{W_f}{W_p + W_f} \times 100 \quad (1)$$

where  $W_p$  and  $W_f$  represent the weight of polymer and the filler, respectively. The composite films were prepared for different concentrations viz. 0, 10, 20, 30, 40, and 50 wt %.

### Experimental techniques

X-ray diffraction (XRD) was performed for diffraction angles  $2\theta$  varying from  $4^\circ$  to  $80^\circ$  using Siemens type F diffractometer. The whole experiment used  $\text{CuK}\alpha$  radiation ( $\lambda = 1.5406 \text{ \AA}$ ). The XRD patterns were recorded at room temperature. Differential scanning calorimetry (DSC) was carried out using an equipment type (GDTD16-Setaram). The DSC curves were recorded in the temperature range of  $30\text{--}400^\circ\text{C}$  for heating rate  $10^\circ\text{C}/\text{min}$  under continuous nitrogen gas flow. The infrared spectrophotometer (Perkin Elmer 833) was used for measuring the FTIR spectra in the wavenumber range of  $400\text{--}4000 \text{ cm}^{-1}$ . The dielectric measurements were carried out at room temperature using an AC impedance bridge (WAYNE KERR precision component analyzer model 6440B) in frequency ranging from 20 Hz to 3 MHz. By sandwiching the sample between two copper electrodes of 1 cm diameter, the capacitance  $C$ , resistance  $R$ , and impedance  $Z$  were recorded for different frequencies. Using the capacitance values  $C$ , the dielectric constant is calculated with the relation:

$$\epsilon' = \frac{C}{C_0} \text{ and } c_0 = \epsilon_0 \frac{A}{d} \quad (2)$$

where  $d$  is the thickness of the sample,  $A$  is the area of the electrode, and  $\epsilon_0 = 8.854 \times 10^{-12} \text{ F/m}$  is the permittivity of free space. The AC conductivity was calculated using the relation:

$$\sigma_{ac} = 2\pi f \epsilon_0 \epsilon' \tan \delta \quad (3)$$

where  $f$  is the frequency,  $\epsilon'$  is the dielectric constant, and  $\tan \delta$  is the dielectric loss. The dc magnetic sus-

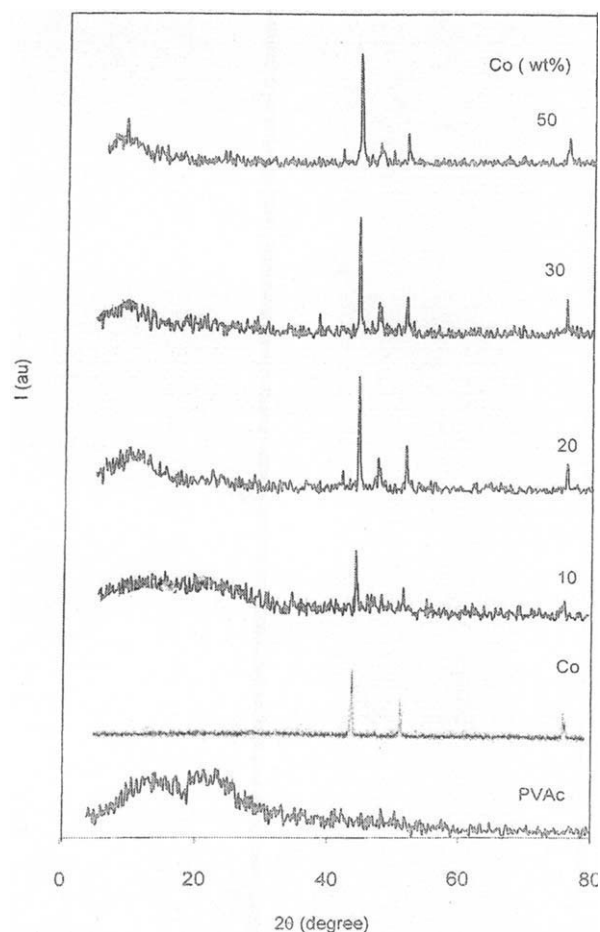


**Figure 1** XRD patterns of unfilled PVAc, Co, and PVAc/Co composite films.

ceptibility was measured using a Faraday pendulum balance technique, which provides accuracy better than  $\pm 3.0\%$ . The electron spin resonance (ESR) spectra were recorded on JEOL spectrophotometer (type JES-FE2XG) at frequency of 9.5 GHz using 1,1-diphenyl-2-picrylhydrazyl (DPPH) as a calibrant.

## RESULTS AND DISCUSSION

### X-ray diffraction

Figure 1 depicts XRD patterns of the pure PVAc, Co, and PVAc/Co composite films. The XRD pattern of pure PVAc shows two broad peaks at angles  $2\theta = 14^\circ$  and  $22^\circ$ , which reveal the amorphous nature of the PVAc.<sup>7</sup> Spectrum of Co metal also shows some intense peaks at angles  $2\theta = 44.5^\circ$ ,  $51.6^\circ$ , and  $76^\circ$ , which correspond to the crystalline phases of the Co.<sup>8</sup> The XRD patterns of PVAc/Co composites, at filling levels 10, 20, 30, and 50 wt % of Co, are presented in Figure 1. The incorporation of Co into the PVAc matrix causes an increase in amorphous character of the PVAc, whereas only one broad peak was observed at higher filling levels. This behavior demonstrates that the interaction between the filler and

the polymer takes place in the amorphous region.<sup>7</sup> For filling levels 20, 30, and 50 wt %, there are new peaks observed at  $2\theta = 41.7^\circ$  and  $47.5^\circ$  suggesting that the new phases are formed due to the crosslinking of PVAc with Co.<sup>9</sup> There is also a new peak at  $2\theta = 38.4^\circ$  for filling level 30 wt %, which may indicate  $\text{Co}_3\text{O}_4$  oxide.<sup>10</sup>

It is quite clear that the incorporation of Co to the polymeric matrix raises the intensity of the reflection at  $2\theta = 44.5^\circ$ . For this purpose, the peak intensity,  $I$ , for the composites was determined and tabulated in Table I. It is clear that the intensity of the crystalline peak increases by the Co content. The present findings may be attributed to the increase in the mode of intercalation of Co with the PVAc chain.<sup>11</sup>

The above analysis concludes that the interaction between Co ions with different structural forms, tetrahedral and octahedral, and PVAc chain takes place in the amorphous region.

### Differential scanning calorimetry

DSC was performed to observe the change in transition temperature caused by adding Co. DSC thermograms of pure PVAc as well as PVAc/Co composite films were depicted in Figure 2. The scan of pure PVAc shows the glass transition temperature ( $T_g$ ) at about  $43^\circ\text{C}$ ,  $\alpha$ -relaxation temperature ( $T_\alpha$ ) at about  $83^\circ\text{C}$ , and decomposition temperature ( $T_d$ ) at about  $322^\circ\text{C}$ . The dependence values of  $T_g$ ,  $T_\alpha$ , and  $T_d$  on filling levels were tabulated in Table I. It is observed that  $T_g$  shows a decrease and then increase in higher temperatures with rising Co content. This indicates that the Co prevented the segmental motion of the polymer chains. As more Co exists, more interaction between polymer chain and Co ions ( $\text{Co}^{2+}$ ,  $\text{Co}^{3+}$ ) becomes stronger. These strong interactions limit the movement of the polymer chain segments due to increase rigidity structure of polymer.<sup>12</sup> Moreover, the thermograms reveal that the PVAc decomposed at  $322^\circ\text{C}$  corresponding to the elimination of acetic acid and decomposition of polyene sequence. The dependence of the thermal decomposition temperature on filling levels shows two decomposition temperatures ( $T_{d1}$  and  $T_{d2}$ ) for filling level  $>10$  wt %.

**TABLE I**  
The Filling Level Dependence of the Peak Intensity ( $I$ ), Glass Transition Temperature ( $T_g$ ), Relaxation Temperature ( $T_\alpha$ ), and Decomposition Temperatures ( $T_{d1}$  and  $T_{d2}$ )

Co (wt %)	$I$	$T_g$ ( $^\circ\text{C}$ )	$T_\alpha$ ( $^\circ\text{C}$ )	$T_{d1}$ ( $^\circ\text{C}$ )	$T_{d2}$ ( $^\circ\text{C}$ )
Unfilled	–	43	83	322	–
10	30	36	82	319	–
20	50	40	83	316	354
30	56	46	81	319	358
50	57	54	82	323	360

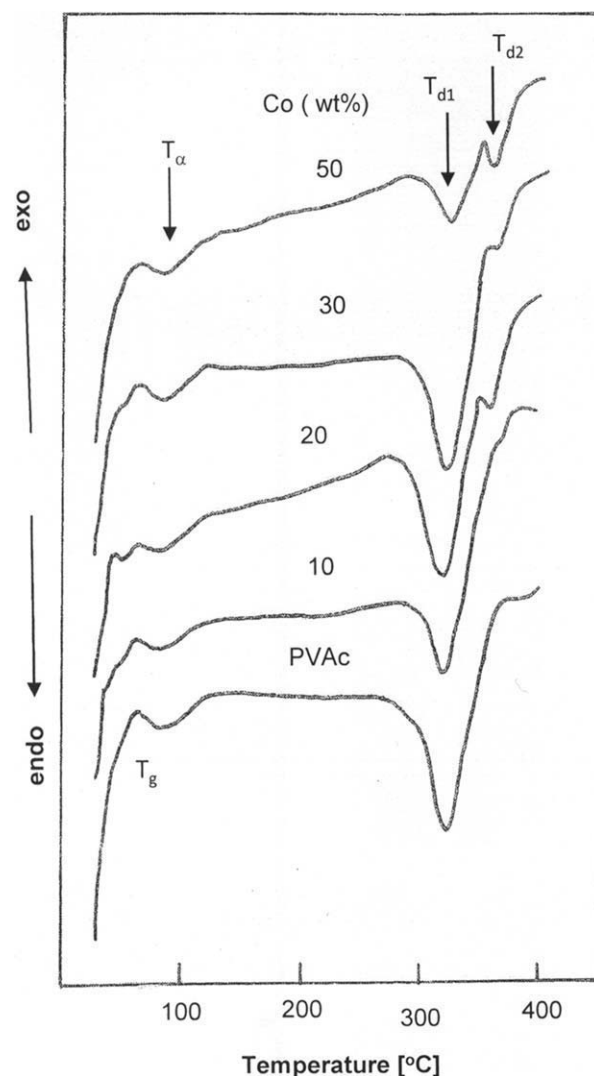


**Figure 2** DSC thermo-grams of pure PVAc and PVAc/Co composite films.

The first one ( $T_{d1}$ ) is nearly unchanged, but the second one ( $T_{d2}$ ) which corresponds to the complete decomposition of Co carbonate and hydroxide,<sup>13</sup> increases with Co content increase indicating that the incorporation of Co particles increases the thermal stability of crosslinked PVAc films.

### FTIR spectroscopy

The FTIR spectra of pure PVAc as well as PVAc/Co composite films are shown in Figure 3. The FTIR spectrum of PVAc shows the stretching vibration of  $-\text{OH}$  at  $3644$  and  $3475\text{ cm}^{-1}$ . The appearance of the strong band at  $1725\text{ cm}^{-1}$  is attributed to  $\text{C}=\text{O}$  stretching. The characteristic peaks at  $1259$  and  $960\text{ cm}^{-1}$  are due to an asymmetric and symmetric  $-\text{C}-\text{O}-\text{C}-$  stretching, respectively.<sup>14</sup> Effectively, Figure 3 shows that when the Co was added to the PVAc, two alternations of the original spectrum of PVAc were observed. The first is the shift in

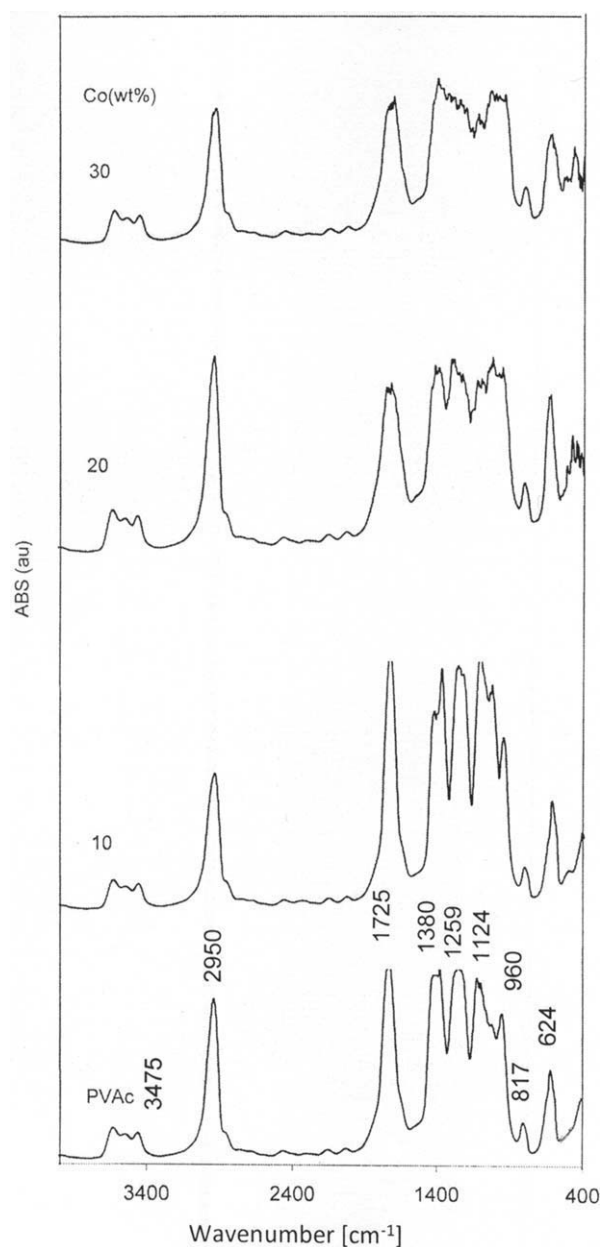


**Figure 3** FTIR spectra of unfilled PVAc and PVAc filled with different filling levels of cobalt.

frequency of the carbonyl and ester groups of the composites when compared with the unfilled PVAc, which indicates the interaction between the filler and the polymeric matrix. The second is the appear-

ance of new bands in the range of 400–500  $\text{cm}^{-1}$ . These new bands may be correlated likewise to defects induced by charge transfer reaction between the filler and the polymeric matrix indicating the formation of the Co oxide. Similar results were obtained by Nicho and Hu.<sup>14</sup> The observed peak at 542  $\text{cm}^{-1}$  corresponding to the  $\nu(\text{Co}-\text{O})$  mode confirm the formation of  $\text{Co}_3\text{O}_4$  spinel oxide.<sup>15</sup>

The shift in frequency is correlated with force constant and bond length. The force constant values can be calculated from the expression<sup>16</sup>

$$\nu = \frac{1}{2\pi c} \sqrt{\frac{k}{M}} \quad (4)$$

where  $\nu$  is the wavenumber,  $c$  is the velocity of light,  $k$  is the force constant, and  $M$  is the reduced mass. The values of the force constant are listed in Table II. It is interesting to note that the force constant increases with increasing Co content. This increase in the force constant is due to the interaction of the Co with the polymer chain which disturbs the delocalization of electrons in the carbonyl and ester groups.

### Dielectric studies

#### Dielectric constant ( $\epsilon'$ )

Figure 4 shows the measured dielectric behavior of the pure PVAc and the composite samples as a function of frequency at room temperature. It was observed that the dielectric permittivity decreases as frequency increases showing usual dielectric dispersion behavior. The decrease in permittivity is rapid at lower frequencies and slower at higher frequencies. Similar behavior was observed in other materials.<sup>17</sup> Generally, the dielectric properties of the polar polymers depend on whether the dipoles are attached to the main chain or not, and the dipole polarization depends on segmental mobility, which is low at temperatures below the glass transition temperature. In view of this, the observed variation of dielectric constant is understood by invoking the Maxwell-Wagner-Sillars effect of polarization.<sup>18</sup> Accordingly, the enhancement in the dielectric properties is attributed to the interfacial polarization: a phenomenon that

**TABLE II**  
The Filling Level Dependence of the Force Constant  $k$  for C=O and C—O—C Band Variations in PVAc/Co Composites

Co (wt %)	C=O band variations		C—O—C band variations	
	Wavenumber ( $\text{cm}^{-1}$ )	Force constant (N/cm)	Wavenumber ( $\text{cm}^{-1}$ )	Force constant (N/cm)
Unfilled	1725	12.01	1259	6.4
10	1725	12.01	1272	6.53
20	1750	12.37	1307	6.9
30	1775	12.72	1309	6.92

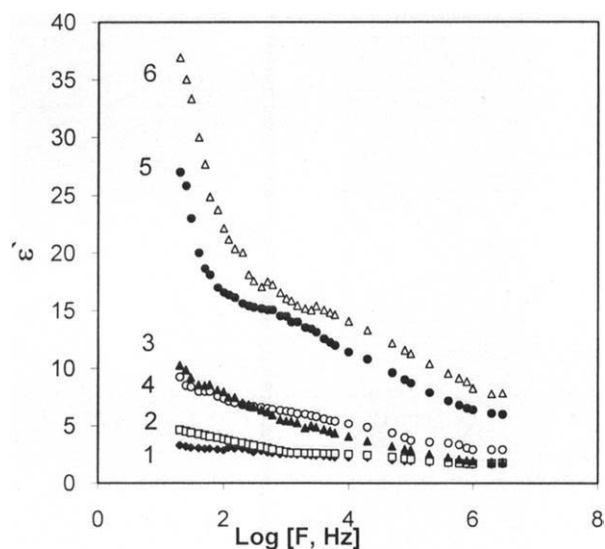


**Figure 4** Variation of  $\epsilon'$  with frequency for: (1) PVAc, (2) 10 wt %, (3) 20 wt %, (4) 30 wt %, (5) 40 wt %, and (6) 50 wt %.

appears in heterogeneous media consisting of phases with different dielectric constant and is mainly due to the accumulation of charges at the interfaces. In the present case, like any other polar material, PVAc is a polar polymer where each dipole can act as an electron trap and hence the observed high value of the dielectric constant is understood.

In other words, the decrease in dielectric constant with increase in frequency for all concentrations can be appropriately explained on the basis of charge carriers being blocked at the electrode. This may be attributed to the tendency of dipoles in a macromolecule to orient themselves in the direction of the applied field in the low frequency range. However, as the frequency of the applied field increases, the dipoles will hardly be able to orient themselves in the direction of the applied field, and hence, the value of the dielectric constant decreases at high frequency.<sup>18</sup>

Figure 5 represents the variation of  $\epsilon'$  as a function of weight percentage of Co at room temperature and at certain frequency 10 kHz. It is observed that the dielectric constant of the samples increases with the Co content. This increase can be understood from the polarization of the conductive particles; mobile charges follow the alternating electric field and accumulate at the interfaces between the particles and the insulating matrix. Thus, the electric field inside the particles becomes negligibly small, the polarization is enhanced and the permittivity is increased (Maxwell-Wagner-Sillars) polarization.<sup>19</sup>

#### AC conductivity ( $\sigma_{AC}$ )

The frequency-dependent AC conductivity in the case of disordered materials such as polymers can

arise from interfacial polarization at contacts, grain boundaries, and other inhomogeneities present in the sample.

The variation of AC conductivity ( $\sigma_{AC}$ ) as a function of frequency is represented in Figure 6. It is clear that the logarithm  $\sigma_{AC}$  shows an increasing trend with the increase in frequency for all samples. This behavior is related to the Maxwell-Wagner type. It is known that the solid consisting of phases with different conductivities influences the overall conductivity of the material, which increases with frequency. At lower frequencies, the grain boundaries are more active, and hence, the hopping of Co ions is less at lower frequencies. As the frequency of the applied field increases, the conductive grains become more active, thereby increasing the hopping conduction. Similar behavior was reported by Alder and Fienlieb.<sup>20</sup>

Figure 7 shows the behavior of the AC conductivity ( $\sigma_{AC}$ ) as a function of filler concentrations at certain frequency 10 kHz. It was observed that the conductivity is enhanced with the increase in Co concentration till filling level 30 wt %, then slight falls off for more Co content. Generally, the observed enhancement in AC electric conductivity ( $\sigma_{AC}$ ) by increasing the filler content is attributed to the electronic interaction processes taking place in the composites; therefore, the PVAc/Co composite becomes more conductive with the increase in conductive filler content. The main factor influencing the composite conductivity is the concentration of the filler particles. At low filler content, the conducting particles are separated and the electric charge may flow by means of hopping through a nonconducting medium between the neighboring particles. The fall off in conductivity beyond 30 wt % is due to the fact that  $\text{Co}^{2+}$  must be partly changed to  $\text{Co}^{3+}$ . A greatly increased conductivity was observed

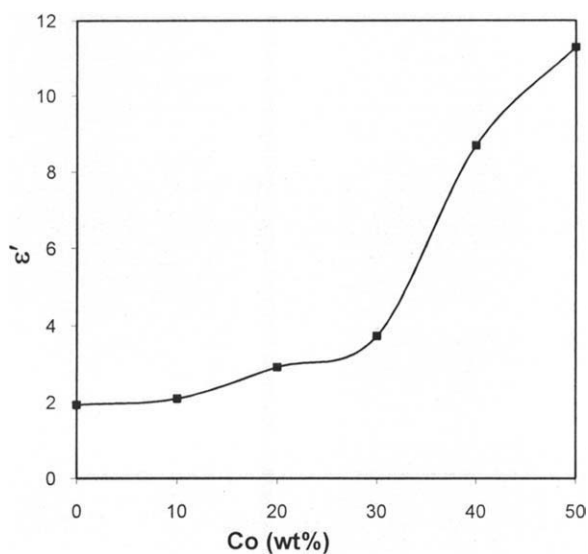


**Figure 5** Variation of  $\epsilon'$  with Co content at  $f = 10$  kHz.

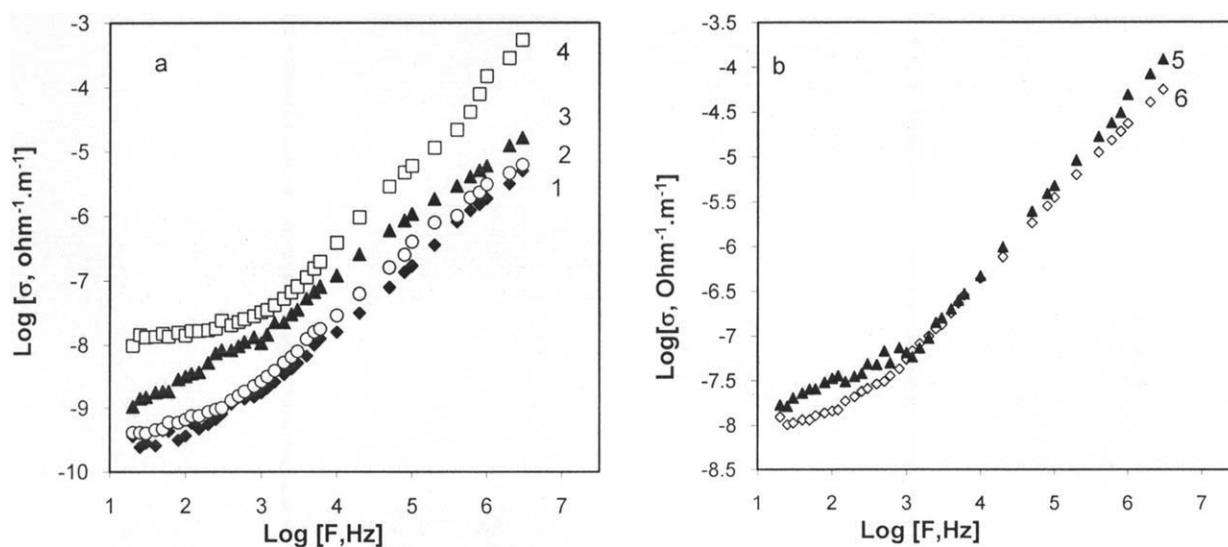


**Figure 6** Frequency dependence of  $\sigma_{AC}$  for (a): (1) PVAc, (2) 10 wt %, (3) 20 wt % and (4) 30 wt %, (b): (5) 40 wt % and (6) 50 wt %.

for filling level 30 wt % due to the dominance of  $\text{Co}_3\text{O}_4$  spinel oxide.<sup>21</sup>

#### DC magnetic susceptibility ( $\chi_{dc}$ )

The dc magnetic susceptibility ( $\chi_{dc}$ ) was measured at room temperature for the prepared PVAc/Co composites. Our experimental values of the dc magnetic susceptibility were used to estimate the effective magnetic moment ( $\mu_{eff}$ ) in Bohr magnetons ( $\mu_B$ ) using the following equation<sup>22</sup>

$$\mu_{eff} = 2.828\sqrt{\chi_{dc}T} \quad (5)$$

where  $T$  is the absolute temperature. The filling level dependence of the effective magnetic moment is

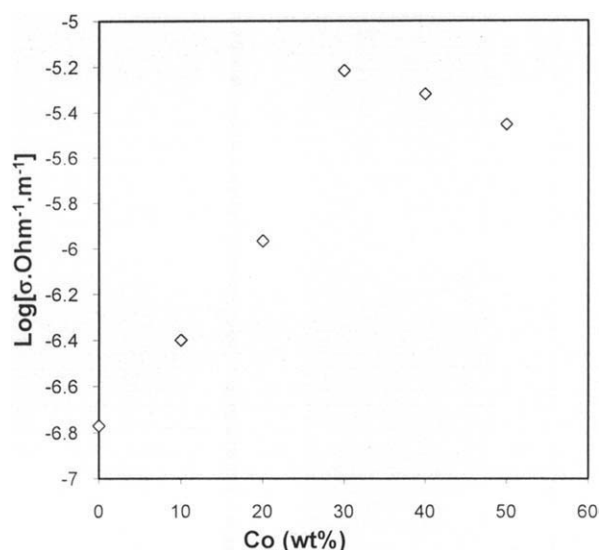


**Figure 7** Dependence of  $\sigma_{AC}$  in PVAc/Co composite films on concentration of cobalt metal at  $f = 10$  kHz.

shown in Figure 8. This behavior shows an increase in the effective magnetic moment from 1.92 to 5.02  $\mu_B$  with increase of Co particles content from 10 to 30 wt %. The increase in magnetization is related to an increase in dipolar interaction among Co particles because particles proximity increases with increase of Co particles in PVAc. It is clear that the order of magnitude of magnetic moment confirms the high spin state of  $\text{Co}^{2+}$  ion.<sup>22</sup> The nonlinear filling level dependence of  $\mu_{eff}$  has indicated that the present system does not show magnetic dilution behavior. It is remarkable that the significant values of  $\mu_{eff}$  indicate that the present filler generally increases the magnetic response of composites. It is well known that the magnetization of magnetic materials is dependent on the morphology and structure of the

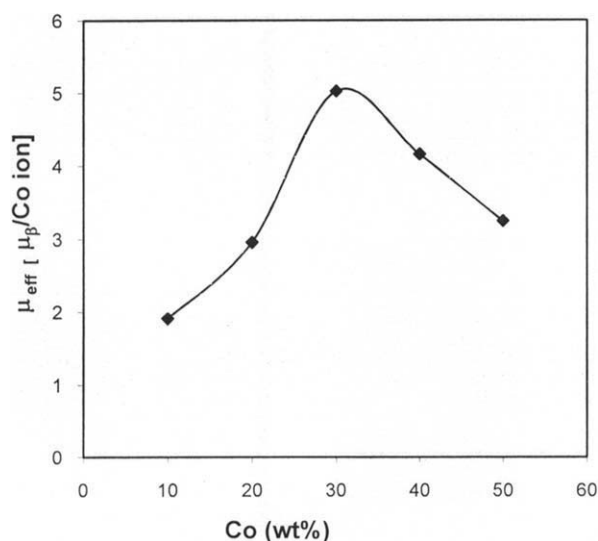


**Figure 8** Dependence of  $\mu_{eff}$  in PVAc/Co composite films on cobalt content.

sample. The lowering of the effective magnetic moment for filling levels more than 30 wt % of Co can be caused by a greater probability to form spinless bipolarons as a result of the electron-phonon intra- and inter-chain interactions.<sup>23</sup> On the other hand, when introducing more than 30 wt % of Co in PVAc,  $\text{Co}^{2+}$  must be changed to  $\text{Co}^{3+}$  which the anisotropy energy of  $\text{Co}^{3+}$  ions is small and orbital angular momentum of these ions is zero.<sup>24</sup>

### Electron spin resonance

Figure 9 shows the ESR spectra of pure PVAc and PVAc/Co composites. The ESR spectra of different filling levels of composites are compared with the unfilled PVAc to establish the influence of Co on molecular mobility. It is observed that the ESR spec-

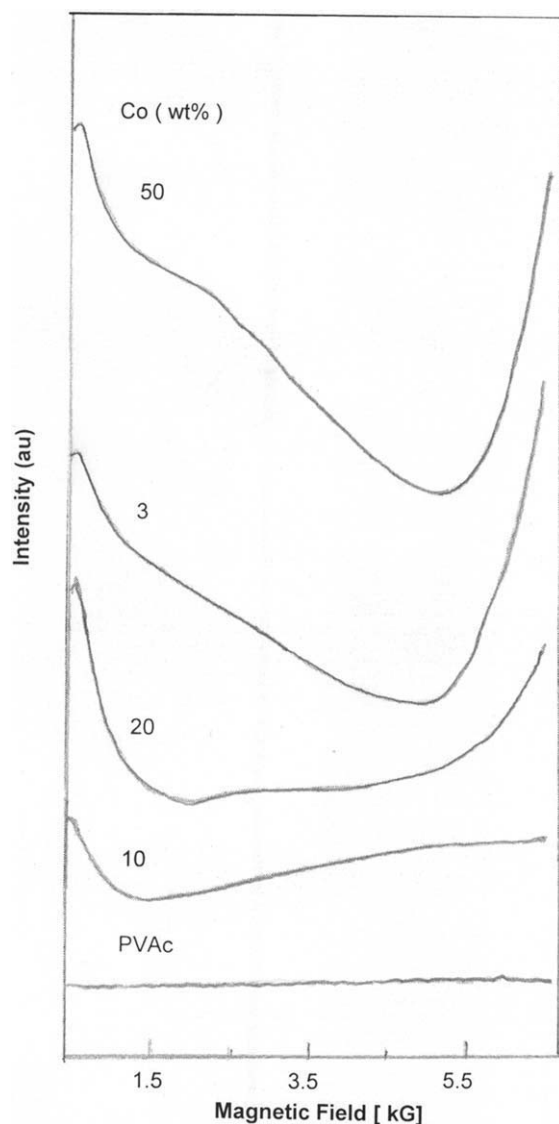


**Figure 9** ESR spectra for various concentrations of cobalt metal of PVAc films at room temperature.

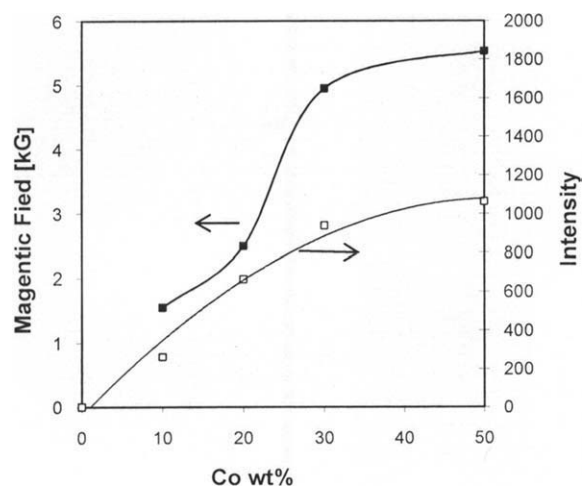


**Figure 10** Dependence of both signal position (■) and signal intensity (□) on concentration of cobalt metal.

trum of unfilled PVAc shows a very weak ESR spectrum assigned to free radicals generated by scission of macromolecular chain during the preparation and processing of the sample. However, the spectra for different filling levels are found to be rather different. Thus, the shape of ESR spectra strongly depends on Co content. Composites spectra are characterized by very broad ESR signal. The broad signal peak like ESR indicates Co clusters inside the PVAc. The filling level dependence of the peak intensity and position are shown in Figure 10. The peak position is shifted to high magnetic fields as Co content increases. The dependence of the intensity of the peak on the filling levels is given by fitting equation

$$I = 0.42 W^2 + 43.7 W - 45.4 \quad (6)$$

where  $I$  is the peak intensity and  $W$  is the filling level. The intensity of the peak is correlated to the number of spin.<sup>25</sup> Thus, the spin concentration increases as Co content increases.

### CONCLUSIONS

PVAc/Co composites films were prepared with various compositions by solvent casting method. Influence of Co addition on structure, dielectric, and magnetic properties of PVAc were studied. XRD patterns reveal the increase of the amorphous nature of PVAc after incorporation of Co. Also, Co oxides were formed at higher Co content. DSC measurements reveal an increase in  $T_g$  with the increase in Co content. FTIR spectra show molecular interactions between the functional groups of PVAc and the Co ions leading to Co oxide formation. The dielectric dispersion with frequency was observed and explained on the basis of polaron and bipolaron

hopping mechanism, which is responsible for conduction and polarization. The dielectric constant shows an increasing trend with increasing Co content. AC conductivity measurements suggest that the conduction in the present system may be due to the polaron hopping mechanism. Effective magnetic moment measurement reveals that the present filler increases the magnetic response of the polymer. Finally, we would like to mention that the results of dielectric, AC conductivity, and magnetic properties show a strong dependence on the weight percentage of Co in PVAc matrix. The composite sample at 30 wt % shows maximum response of AC conductivity and magnetic moment. This dependence makes the prepared composite film candidate for more applications in electric and magnetic sensor.

The author thanks to Professor Magdy M. Ghannam, Department of Physics and Astronomy, College of Science, King Saud University, Kingdom of Saudi Arabia, for his kind assistance, support, and encouragements. He also thanks Dr. Mahmoud Abdelhaleem, PhD in Linguistics, Department of Arts and Education, Riyadh Community College, King Saud University for language revision.

## References

1. Kumar, G. N. H.; Rao, J. L.; Gopal, N. O.; Narasimhulu, K. V.; Chakradhar, R. P. S.; Rajulu, A. V. *Polymer* 2004, 45, 5407.
2. Michaeli, W.; Pfeifferkorn, T. G. *Polym Eng Sci* 2009, 49, 1511.
3. Bard, W. S.; Pakade, S. V.; Yawale, S. P. *J Non-Cryst Solids* 2007, 353, 1460.
4. Bhargav, P. B.; Mohan, V.; Sharma, A. K.; Rao, V. V. R. *Curr Appl Phys* 2009, 9, 165.
5. Abdelaziz, M.; Abdelrazek, E. M. *Phys B* 2004, 349, 84.
6. Choi, C. S.; Park, B. J.; Choi, H. J. *Diamond Related Mater* 2007, 16, 1170.
7. Baskaran, R.; Selvasekarapandian, S.; Kuwata, N.; Awamura, J. K.; Hallori, T. *J Phys Chem Solids* 2007, 68, 407.
8. Yao, Z.; Zhu, A.; Chen, J.; Wang, X.; Au, C. T.; Shi, C. *J Solid State Chem* 2007, 180, 2635.
9. El-Tantway, F.; Abdelkader, K. M.; Kaneko, F.; Sung, Y. K. *Eur Polym J* 2004, 40, 415.
10. Tang, C. W.; Wang, C. B.; Chien, S. H. *Thermochem Acta* 2008, 473, 68.
11. Jia, X.; Li, Y.; Zhang, B.; Cheng, Q.; Zhang, S. *Mater Res Bull* 2008, 43, 611.
12. Zulfikar, M. A.; Mohammad, A. W.; Kadhum, A. A.; Hilal, N. *Mater Sci Eng A* 2007, 452, 422.
13. Gulari, E.; Culdur, G.; Srivannavit, S.; Osuwan, S. *Appl Catal A* 1999, 185, 147.
14. Nicho, M. E.; Hu, H. *Sol Energy Mater Sol Cells* 2000, 63, 423.
15. Hong, L.; Jiang, J. *Power Technol* 2009, 195, 11.
16. Stuart, B. *Infrared Spectroscopy: Fundamentals and Applications*; John Wiley & Sons, Ltd, 2004; Chapter 1.
17. El-Shahawy, M. A.; Elkholy, M. M. *Eur Polym J* 1994, 30, 259.
18. Bhajantri, R. F.; Ravindrachary, V.; Harisha, A.; Ranganathaiah, C.; Kumaraswamy, G. N. *Appl Phys A* 2007, 87, 797.
19. Baskaran, R.; Selvasekarapandian, S.; Kuwata, N.; Kawamura, J.; Hattori, T. *Mater Chem Phys* 2006, 98, 55.
20. Alder, D.; Fienlieb, J. *Phys Rev B* 1970, 2, 3112.
21. Kambale, R. C.; Shaikh, P. A.; Bhosale, C. H.; Rajpure, K. Y.; Kolekar, Y. D. *Smart Mater Struct* 2009, 18, 5014.
22. Nicholls, D. *Complexes and First Row Transition Elements*; Whitefriars Press Ltd.: London, 1974; p 187.
23. Cik, G.; Sersen, F.; Dihan, L. *J Magn Magn Mater* 2000, 208, 78.
24. Zhao, M.; Peng, H.; Han, Z. *Sens Actuators B* 2008, 129, 953.
25. Abdelaziz, M. *J Appl Polym Sci* 2008, 108, 1013.